Mathematical Model of the Liquid Membrane Extractive Column. Sensitivity to Operating Parameters

DANIEL DINCULESCU*, VASILE LAVRIC
University Politehnica of Bucharest, Chemical Engineering Department, , Polizu 1-7, 011061, Bucharest, Romania

The extraction-back extraction column of low concentration species by means of an organic closed loop flow, considered as liquid membrane, was modelled then simulated, using some simplifying assumptions. The main hypotheses are: the aqueous phase is perfectly mixed, the drops of the organic phase are lumped into a plug-flow inner cylinder co-axial with the aqueous phase, and the organic phases under the sieve and on the top of the column are perfectly mixed also. The dynamic model of the extraction-back extraction column is, then, applied to the recovery of the hydrocarboxylic acids. The mathematical model, reduced through orthogonal collocation to a system of ordinary differential equations, was solved using a self-adaptive (RK)-type method. Its validation was done based on batch experimental data; the optimal model parameters (the specific mass transfer coefficients for both extraction and back-extraction zones), ensuring the agreement with the experiment, were found by means of a modified genetic algorithm technique. Then, a sensitivity analysis was done, to grasp the behaviour of the system with respect to the main operating parameters - the organic flow in the closed loop, the partition coefficient and the buffer volume.

Keywords: liquid membrane, liquid-liquid extraction, hydrocarboxylic acids, orthogonal collocation, membrane column modelling, genetic algorithm

The possibility of carboxylic acids recovery from aqueous streams such as fermentation broths and wastewaters using liquid membranes is proved to be a valuable technique that increases the concentration of the transported species in the receiver phase [1, 2]. Experimental results for liquid-liquid equilibrium involved in the extraction of carboxylic acids show that non-polar extractants are characterized by small partition coefficients due to the great affinity of acids toward the water [3]. Such solvents make the extraction inefficient especially when applied to dilute acid solutions. To overcome this, polar solvents characterized by higher distribution ratios are needed, despite their drawback of mixing with water in really significant proportions.

The liquid membrane transport is modelled using one of the following approaches [4]: ordinary permeation, facilitated transport (type-II-facilitated transport is the most studied case [5, 6]) and molecular pumping. Recent works take into account undesirable intrinsic phenomena such as swelling and breakage of the drops, whose distribution have to be controlled during the reactive extraction process [7]. Few works present a complete mathematical model including both processes implied by a liquid membrane: the extraction and the back extraction [8, 9].

The possibilities associated to the use of liquid membrane technologies were heavily investigated in literature. The designing and operating costs of the plants based upon liquid membrane technologies are lower than the costs of the plants using the classical methods to achieve the same goal [10]. Nevertheless few papers published in the open literature approach the design of equipment using liquid membranes. The majority of these papers consider the modelling, simulation and control of classical liquid-liquid extraction columns or batch agitated liquid-liquid extractors [11 - 13].

The mathematical model of an innovative single column, designed for extraction and back extraction cascade, is presented in this work. The column, divided by a sieve plate, allows a solute extraction with some polar organic solvent (i.e., a carboxylic acid), dispersed as ascending drops, from the aqueous continuous phase in the inferior half of the device. In the superior half, an inverse process leads to a back extraction from the same organic, also dispersed as ascending drops, to the aqueous phase. The mathematical model, based upon a simplified circulation model for both phases, organic and aqueous, considers the thermodynamic equilibrium at the liquid-liquid interface, and the unsteady state mass conservation of the transported species, including the inter-phase mass transfer. Thus, it encapsulates information related to the operating time and process parameters, unfolding the dynamic behaviour of the extraction - back extraction column.

Experimental details

Reagents and solutions

Distilled water (previously saturated with organic) was used during the experimental part of this work. Acetic acid, the transported species, was supplied by Chimopar S.A. Bucharest and the solvent (n-octanol) by Merck Co. The aqueous solutions were prepared by diluting acid solution with distilled water without pH adjustment, since this would have had as result a possible voluntary contamination of the solution. The organic solvent was also saturated with water prior to be used.

Experimental procedure

The acid extraction from aqueous solution was performed in the experimental setup presented in Figure 1a. The carrier used is an organic solvent which is considered as a liquid membrane, distributed along the column in various ways. The glass column has 660 mm height and 40 mm inner diameter. The pump (1) feeds the organic phase into the column, through a nozzle (2) mounted at the bottom of the extraction zone (5). The

* *email: d_dinculescu@chim.upb.ro*

nozzle disperses the organic into small droplets (5'), which rise through the aqueous phase and coalesce under the sieve forming a continuous layer (6). This way, the aqueous phase of the bottom of the column (extraction zone - 5) is completely separated from the aqueous phase of the top (back extraction zone - 8). Due to the incompressible nature of the liquids, when the organic enters the extraction zone, new droplets of organic phase (8') are formed into the back-extraction region, due to the sieve which acts like a nozzle. The aforementioned droplets rise to the top of the column where they coalesce again into a bulk (10). From here, the organic is recycled to the bottom of the column after being previously collected into a buffer vessel (11). The carrier (droplets of organic phase) will extract the organic acid present in the extraction zone and will transport it into the back-extraction region of the column, provided that the solubility constraints are met. In this experimental work, the transported chemical species was acetic acid and the carrier was *n*-octanol.

The concentration of the solute (acetic acid) in the continuous phase of the extraction zone was determined by titration, removing small samples of liquid at several time-intervals, care being taken not to disturb the hydrodynamics of the column. Details regarding all the steps of the experimental protocol are presented in [14].

The mathematical model

Main hypothesis

The mathematical model was developed under the following simplifying assumptions:

-the dispersed organic phase was lumped into a cylinder, coaxial with and surrounded by the aqueous phase (Figure 1b), for both halves of the column;

-the plug-flow model for the organic phase circulation through cylinders was assumed, taking into account the lack of the coalescence - dispersion phenomena between the ascending drops, which are seen as perfectly mixed; if the internal drop circulation in not so intense, the model can easily be extended to take this into consideration through axial dispersion;

-both zones with carboxylic acid aqueous solutions were assumed perfectly mixed; if the circulating cells induced by the upward movement of the drops do not extend to the whole aqueous regions, a more suitable model could be used, such as a cascaded perfectly mixed cells with small interconnected flows;

-the organic layers under the sieve and on the top of the column and the buffer vessel are considered perfectly mixed;

-the pipes' volume was neglected;

-the process was regarded as isothermal;

Mathematical model development

Taking into account the above mentioned assumptions, the equations of the mathematical model, derived from mass balances for the carried species, are:

- extraction zone

- organic phase

$$\underbrace{\frac{\partial C_{o,ex}}{\partial t}}_{\text{Solute accumulation into the carrier}} + \underbrace{u_{ex}\cdot\frac{\partial C_{o,ex}}{\partial z_{ex}}}_{\text{Solute convective molar flow}} - \underbrace{\frac{n_{A,ex}}{D^{o}_{eq}}}_{\text{Solute inlet flow through interface}} = 0 \qquad (1)$$

- aqueous phase

$$\underbrace{V_a\cdot\frac{dC_{A,ex}}{dt}}_{\text{Solute accumulation into aqueous phase}} + \underbrace{n_{A,ex}\cdot\left(A_{ex}+A_{sup,ex}\right)}_{\text{Solute outlet flow through interface}} = 0 \qquad (2)$$

- extraction - back extraction separation zone:

$$\underbrace{V_{o,ex-bk}\cdot\frac{dC_{o,ex-bk}}{dt}}_{\text{Solute accumulation into the carrier under the sieve}} - \underbrace{D_V\cdot\left(C_{o,ex}-C_{o,ex-bk}\right)}_{\text{Net solute flow}} - \underbrace{n_{A,ex}\cdot A_{sup,ex}}_{\text{Solute inlet flow through the interface}} = 0 \qquad (3)$$

- back extraction zone

- organic phase

$$\frac{\partial C_{o,bk}}{\partial t} + u_{re}\cdot\frac{\partial C_{o,bk}}{\partial z_{bk}} + \frac{n_{o,bk}}{D^{o}_{eq}} = 0 \qquad (4)$$

- aqueous phase:

$$V_{a,bk}\cdot\frac{dC_{A,bk}}{dt} - n_{o,bk}\cdot\left(A_{bk}+A_{sup,bk}\right) = 0 \qquad (5)$$

- top of the column

$$V_{o,f}\cdot\frac{dC_{o,f}}{dt} - D_v\cdot\left(C_{o,bk}-C_{o,f}\right) + n_{o,bk}\cdot A_{sup,bk} = 0 \qquad (6)$$

- buffer vessel

$$V_{o,f}\cdot\frac{dC_{o,f}}{dt} - D_v\cdot\left(C_{o,bk}-C_{o,f}\right) + n_{o,bk}\cdot A_{sup,bk} = 0 \qquad (7)$$

In equations (1) and (4), the equivalent diameter is the same since the volume flow is conserved

$D_v = \left(D^{o}_{eq,ex}\right)^2\pi u_{ex}/4 = \left(D^{o}_{eq,bk}\right)^2\pi u_{bk}/4 = \left(D^{o}_{eq}\right)^2\pi u/4$ and $u_{ex} = u_{bk} = u$ due to the almost identical physical properties.

The model takes also into account the supplemental mass transfer between the aqueous and the organic layers (fig. 1a, 5⟶6 and 8⟶10), as written in equations (2), (3), (5) and (6) under the notation A_{sup} for the supplemental mass transfer area.

The initial and boundary conditions for the system are:

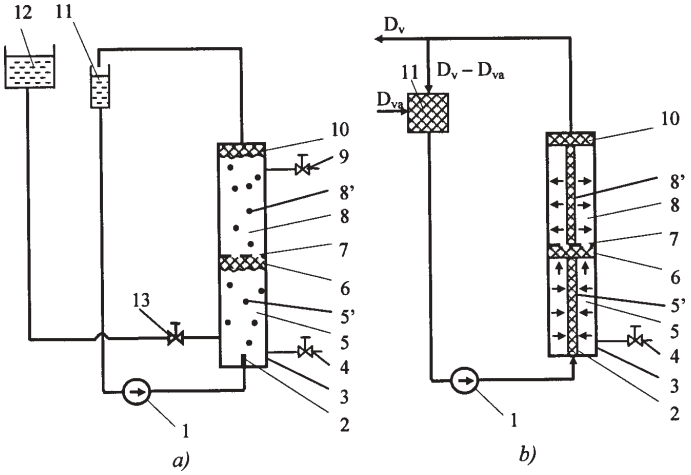

Fig. 1. The experimental set-up a) Schematic diagram; b) The two phase circulation model
1-pump; 2-nozzle; 3-glass column; 4-sample tap; 5-aqueous phase (extraction zone); 5'-organic phase; 6-organic layer; 7-sieve; 8-aqueous phase (back extraction zone); 8'-organic phase; 9-sample tap; 10-organic layer; 11-buffer vessel; 12-water feed vessel; 13-water filling tap

$$t=0;\ z_{ex}\geq 0;\ C_{A,ex}=C_{A,ex}^{in};\ C_{o,ex}=C_{o,f}^{in};\ C_{o,ex-bk}=C_{o,f}^{in}$$

$$C_{o,bk}=C_{o,f}^{in};C_{A,bk}=C_{A,bk}^{in};\ C_{o,f}=C_{o,f}^{in} \quad (8)$$

$$t>0;\ z_{ex}=0;\ C_{o,ex}=C_{o,f}$$

The mathematical model (1÷7) together with its conditions (8) can be render dimensionless using the reference variables $C_{A,ex}^{in}$, $\bar{t}$, H_{ex}, H_{bk}:

$$\frac{\partial \Gamma_{o,ex}}{\partial \tau}+\frac{1}{\alpha}\cdot\frac{\partial \Gamma_{o,ex}}{\partial \zeta_{ex}}=\left(\frac{\Gamma_{A,ex}}{K_{eq}}-\Gamma_{o,ex}\right)\cdot K_{o,ex} \quad (9)$$

where

$$K_{o,ex}=\frac{\bar{t}}{D_{ech}^{o}\cdot\left(\frac{1}{K_{eq}\cdot k_{a,ex}}+\frac{1}{k_{o,ex}}\right)}$$

$$\frac{d\Gamma_{A,ex}}{d\tau}=-\left(\frac{\Gamma_{A,ex}}{K_{eq}}-\Gamma_{o,ex}\right)\cdot K_{ex,a}\cdot\left(\frac{\delta_{ex}}{1-\delta_{ex}^{2}}+\frac{1}{s_{ex}}\right) \quad (10)$$

where:

$$K_{ex,a}=\frac{4\cdot\bar{t}}{D_c\cdot\left(\frac{1}{K_{eq}\cdot k_{a,ex}}+\frac{1}{k_{o,ex}}\right)} \text{ and } s_{ex}=D_c\cdot H_{ex}$$

$$\frac{d\Gamma_{o,ex-bk}}{d\tau}=\frac{\Gamma_{o,ex}-\Gamma_{o,ex-bk}}{\beta}+\left(\frac{H_{A,ex}}{K_{eq}}-\Gamma_{o,ex-bk}\right)\cdot K_{o,ex-bk} \quad (11)$$

where

$$K_{o,ex-re}=\frac{\left(1-\delta_{ex}^{2}\right)\cdot\bar{t}}{\left(\frac{1}{K_{eq}\cdot k_{a,ex}}+\frac{1}{k_{o,ex}}\right)\cdot H_{o,ex-bk}}$$

$$\frac{\partial \Gamma_{o,bk}}{\partial \tau}+\frac{1}{\gamma}\cdot\frac{\partial \Gamma_{o,bk}}{\partial \zeta_{bk}}=\left(\Gamma_{A,bk}-K_{eq}\cdot\Gamma_{o,bk}\right)\cdot K_{o,bk} \quad (12)$$

where

$$K_{o,bk}=\frac{\bar{t}}{D_{ech}^{o}\cdot\left(\frac{K_{eq}}{k_{o,bk}}+\frac{1}{k_{A,bk}}\right)}$$

$$\frac{d\Gamma_{A,bk}}{d\tau}=\left(K_{eq}\cdot\Gamma_{o,bk}-\Gamma_{A,bk}\right)\cdot K_{bk,a}\cdot\left(\frac{\delta_{bk}}{1-\delta_{bk}^{2}}+\frac{1}{s_{bk}}\right) \quad (13)$$

where

$$K_{re,a}=\frac{4\cdot\bar{t}}{D_c\cdot\left(\frac{K_{eq}}{k_{o,bk}}+\frac{1}{k_{A,bk}}\right)}$$

$$\frac{d\Gamma_{o,f}}{d\tau}=\frac{\Gamma_{o,bk}-\Gamma_{o,f}}{\delta_{bk}}-\left(\Gamma_{a,bk}-K_{eq}\cdot\Gamma_{o,f}\right)\cdot K_{o,f} \quad (14)$$

where

$$K_{o,f}=\frac{\left(1-\delta_{bk}^{2}\right)\cdot\bar{t}}{H_{o,f}\cdot\left(\frac{K_{eq}}{k_{o,bk}}+\frac{1}{k_{A,bk}}\right)}$$

$$\frac{d\Gamma_{v}^{o}}{d\tau}=\frac{1}{\phi}\cdot\left(\Gamma_{in,v}^{o}-\Gamma_{v}^{o}\right)-\frac{\psi}{\phi}\cdot\Gamma_{in,v}^{o} \quad (15)$$

The dimensionless initial and boundary conditions became:

$$\tau=0;\ \forall\zeta;\Gamma_{A,ex}=1;\Gamma_{o,ex}=\Gamma_{o,ex-bk}=\Gamma_{o,bk}=\Gamma_{A,bk}=\Gamma_{o,f}=0$$

$$\tau>0;\ \zeta=0;\ \Gamma_{o,ex}=\Gamma_{o,f};\Gamma_{o,bk}=\Gamma_{o,ex-bk} \quad (16)$$

The mathematical model described by equations (9) ÷(15) together with the initial and boundary conditions (16) is a hybrid system of partially and ordinary differential equations. The method used for solving this system was firstly to transform it into an ODE system, through orthogonal collocation, then integrating it with a suitable self-adjustable RK-type method, which in our case was RK Fehdberg [16]. For the orthogonal collocation step, a trial function was taken as a series of orthogonal polynomials whose roots are used as collocation points and the dependent variables become the solution values at these collocation points. The spatial derivatives are replaced with weighted sums of the dependent variables [7], thus transforming a (PDE) into a time dependent (ODE). Knowing the relation of derivate approximation into a collocation point "i" $\left(\frac{\partial\Gamma}{\partial\zeta}\right)_i=\sum_{j=0}^{N+1}\left(A_{j,i}\cdot\Gamma_j\right),\ \ i=1,N,$ which enters into the model's equations [15], the discretized form of the mathematical model in the collocation points is:

The extraction zone

- discontinuous organic phase:

$$\frac{d\left(\Gamma_{o,ex}\right)_i}{d\tau}=\left(\frac{\Gamma_{A,ex}}{K_{eq}}-\left(\Gamma_{o,ex}\right)_i\right)\cdot K_{o,ex}-\left(\Gamma_{o,ex}\right)_0\cdot\left(A_{0,i}-\frac{A_{N+1,i}}{A_{N+1,N+1}}\cdot A_{0,N+1}\right)-$$
$$-\sum_{j=1}^{N}\left(\Gamma_{o,ex}\right)_j\cdot\left(A_{j,i}-\frac{A_{N+1,i}\cdot A_{j,N+1}}{A_{N+1,N+!}}\right) \quad (17)$$

- continuous aqueous phase:

$$\frac{d\Gamma_{A,ex}}{d\tau}=-\left(\frac{\Gamma_{A,ex}}{K_{eq}}-\bar{\Gamma}_{o,ex}\right)\cdot K_{a,ex}\cdot\left(\frac{\delta_{ex}}{1-\delta_{ex}^{2}}+\frac{1}{s_{ex}}\right) \quad (18)$$

where $\bar{\Gamma}_{o,ex}=\frac{\sum_{i=1}^{N+1}\left(\Gamma_{o,ex}\right)_i}{N+2}$

The zone under the sieve:

$$\frac{d\Gamma_{o,ex-bk}}{d\tau}=\frac{\left(\Gamma_{o,ex}\right)_{N+1}-\Gamma_{o,ex-bk}}{\beta}+\left(\frac{\Gamma_{A,ex}}{K_{eq}}-\Gamma_{o,ex-bk}\right)K_{o,ex-re} \quad (19)$$

The back extraction zone

- discontinuous organic phase:

$$\frac{d\left(\Gamma_{o,bk}\right)_i}{d\tau}=K_{o,bk}\cdot\left[\Gamma_{A,re}-K_{eq}\cdot\left(\Gamma_{o,bk}\right)_i\right]-\left(\Gamma_{o,bk}\right)_0\cdot\left(A_{0,i}-\frac{A_{N+1,i}}{A_{N+1,N+1}}\right)-$$
$$-\sum_{j=1}^{N}\left(\Gamma_{o,bk}\right)_j\cdot\left(A_{j,i}-\frac{A_{N+1,i}\cdot A_{j,N+1}}{A_{N+1,N+1}}\right) \quad (20)$$

- the continuous aqueous phase:

$$\frac{d\Gamma_{A,re}}{d\tau}=\left(K_{eq}\cdot\bar{\Gamma}_{o,bk}-\Gamma_{A,bk}\right)\cdot K_{bk,a}\cdot\left(\frac{\delta_{bk}}{1-\delta_{bk}^{2}}+\frac{1}{s_{bk}}\right) \quad (21)$$

where $\bar{\Gamma}_{o,bk}=\frac{\sum_{i=1}^{N+1}\left(\Gamma_{o,bk}\right)_i}{N+2}$

The continuous organic layer on the top of the column:

$$\frac{d\Gamma_{o,f}}{d\tau} = \frac{\left(\Gamma_{o,bk}\right)_{N+1} - \Gamma_{o,f}}{\delta} - \left(\Gamma_{A,bk} - K_{eq} \cdot \Gamma_{o,f}\right) K_{o,f} \quad (22)$$

The organic phase from the buffer vessel:

$$\frac{d\Gamma_v^o}{d\tau} = \frac{1}{\phi} \cdot \left[\Gamma_{in,v}^o \cdot (1-\psi) - \Gamma_v^o\right] \quad (23)$$

Results and discussions

Validation of the mathematical model

The validation of the mathematical model was done using own experimental data [14], to identify the unknown parameters resulted from the application of the simplifying assumptions, and the available literature correlations or design data. The partition coefficient for the system acetic acid / *n*-octanol was experimentally found to be 2, at the working temperature, value comparing well with the literature [14]. All other parameters of the mathematical model were computed using the experimental set-up or the operating conditions, except for the partial mass transfer coefficients: $k_{o,ex}$, $k_{A,ex,}$ $k_{o,re}$, $k_{A,re}$. In fact, in order to eliminate the uncertainties associated with the way the interfacial areas between the rising droplets and the stagnant liquid phases were computed, the real adjustable parameters used were the specific partial mass transfer coefficients: $k_{o,ex}$. A_{ex}, $k_{o,re}$. A_{re} and $k_{A,re}$, $A_{A,re.}$ These parameters were regressed against the experimental data [14], the objective function being the usual sum of the squared residuals model-experiment, which had been minimized. Due to the possibility of local extremum existence, when this kind of function is used, we applied an improved variant of Genetic Algorithm (GA) as optimization tool. GA is an evolutionary, direct search technique, based upon the theory of natural selection and the mechanisms of population genetics, that evaluates thousands of possible solutions as it converges to the global optimum. The evolutionary nature of the GA is defined by: the initial population, randomly generated, but containing its characteristic variability; the suitability associated with each individual in the population, assessed according to a fitness function; the survival probability of each individual, proportional to its fitness; the selection of individuals, based on probability, and breeding through a genetic transformation process of cross-over and mutation, ensuring that the solution is not trapped into a local optimum environment [17-19].

Each adjustable parameter was directly encoded into a gene, thus a chromosome with four genes being formed. Each chromosome defines an individual from the population. Initially, a population pool is created, having a convenient number of individuals. The restrictions are coped with naturally, during the population generation, simply eliminating those individuals outside the feasible domain as given in literature [5, 6, 11, 12, 14, 20]. Then, the mathematical model is solved, for each individual (i.e. the four parameters). After that, the individuals are interbreed according to their frequency of selection, using one-point crossover method, and then mutation is applied to randomly selected individuals, thus producing a new generation.

The results obtained are presented in figures 2 and 3, where a comparison model-experiment is made. In both figures, the acetic acid concentration profile in the back extraction zone is also presented, although no experimental data are available for it. The analysis of figures 2 and 3 shows that, due to the transport of the acetic acid from the extraction to the back-extraction zones, its concentration profiles reach an equilibrium value, which increases with the flow rate of the organic liquid membrane. As a matter of fact, the thermodynamic equilibrium in the column is expected to happen when the concentration of the transported species reaches the same value in both extraction and back-extraction zones. This assumption takes into consideration that the two sections of the column have equal volumes of water and disregard the volume of the organic carrier. But, due to the acetic acid entrapped into the liquid membrane (corresponding to its equilibrium concentration, eventually), which is drawn from the extraction zone, the thermodynamic equilibrium of the acetic acid concentration between the extraction and the back-extraction zones will correspond to a little bit higher than 2 value, as can be seen from figures 2 and 3, at the end of the process. An increase towards this later value would be possible only if the organic responsible for the liquid membrane would be saturated with the carried species from the beginning of the transport process. In figure 4 the time profiles of the carried species in the aqueous phase from the extraction zone and the organic under the sieve zone are presented, to show their asymptotic behaviour towards equilibrium; the rate of the process depends upon the carrier flowrate. As expected, the time needed to reach equilibrium decreases as the carrier flowrate increases. This fact, experimentally proved by the growth of the droplets number into both zones of the column, can be explained, on one hand, by the growth of the interfacial area, and in another, by the increase in the mass transfer coefficients, due to the improved hydrodynamics. The turning point towards the asymptote of the concentration profiles near the end of the process suggests that there could be some critical concentration in the back-extraction zone beyond which any attempt to increase it would be

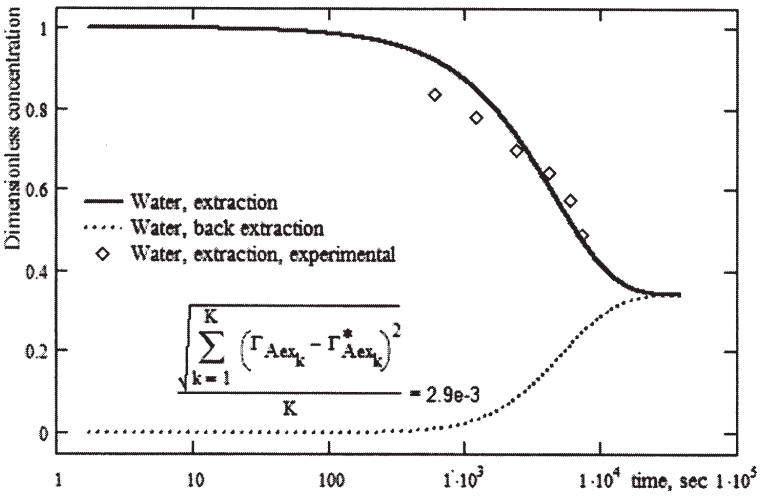

Fig. 2. Mathematical model validation for an organic flowrate of 0.9 cm^3/s - concentration profile of the transported species in the extraction and back-extraction zones of the column (mean dimensionless error is 2.9e-3)

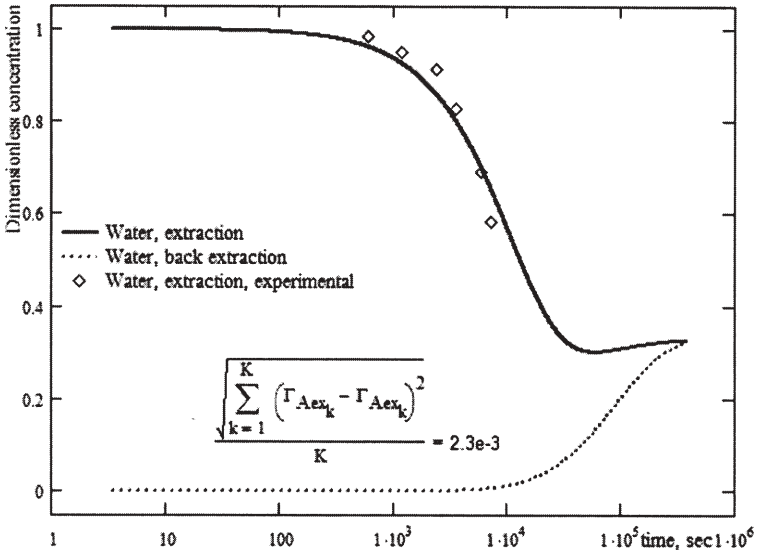

Fig. 3. Mathematical model validation for an organic flowrate of 0.45 cm³/s - concentration profile of the transported species in the extraction and back-extraction zones of the column (mean dimensionless error is 2.3e-3)

uneconomical, due to the mass transfer limitations near thermodynamic equilibrium.

As can be seen from figures 2 and 3, there is a good match between the experimental profiles of the acetic acid in the extraction zone and the ones predicted by the mathematical model, which validate the later. As expected, the discrepancy between the mathematical model and the experiment is higher for the high values of the organic membrane flow (fig. 2), since the orderly structure of the rising droplets can be easily altered by the rotating cells developed in the continuous phase, increasing both the probability of coalescence – breakage phenomena, unaccounted for by the present circulation model and the mass transfer on the aqueous side (fig. 1 and subsequent explanations). These phenomena determined, at the beginning of the process, the high experimental mass transfer rates, which are responsible for the lower organic concentration in the aqueous phase. Since the regression gives a "smooth average" value for the parameters, towards the end of the process the experimental concentrations are a little bit higher than those predicted by the model.

When the organic flow is lower (fig. 3), an interesting phenomenon can be observed for time values beyond 3600 s, that is the experimental mass transfer seems to outcome the performance predicted by the model, quite contrary to the behaviour previously emphasized. This can be the result of the peculiar behaviour of the organic phase stocked under the sieve plate. Although at the beginning of the experiment the organic phase is clear, as the time goes an increasing part tends to emulsify due to the interfacial phenomena whose time scale are in the same order of magnitude as the residence time associated with the volume of this under the sieve plate zone. At the end of the experiment, the emulsified portion of the organic phase is larger than the clear one. At higher carrier flowrates, the emulsification is rather limited since its time scale is larger than that of the residence time of the organic in this peculiar volume (compare with figure 2 for the same process time).

For very long process time, the organic concentration in the aqueous phase decreases towards a minimum which is lower than the equilibrium concentration, then increases towards equilibrium; the carrier acts like a source in the last part of the process – this behaviour will be explained latter. In this time zone, a thorough economic analysis should be done in order to decide if the process can go further or it is beneficial to be stopped here.

Simulations of the liquid membrane extractive column

In order to study the behaviour of the liquid membrane extractive column, some simulations were done, using as parameters the recirculation flow of the organic liquid membrane, the volume of the buffer vessel (fig. 1, entry 11), which takes into account the overall quantity of the organic liquid membrane, and the partition coefficient, which encodes the organic species used as liquid membrane. It has to be mentioned that in all simulations only one operating parameter was modified, all others being kept constant.

Carrier flowrate

The time dependency of the axial concentration profiles for the organic phases along the extraction and back-extraction zones, respectively, are presented in figure 5,

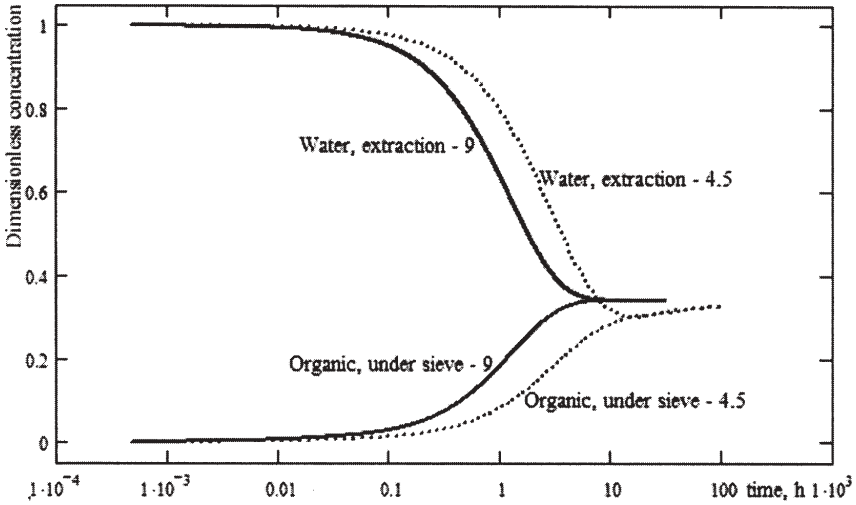

Fig. 4. Concentration profile of the transported species in the continuous phase of the extraction zone and in the organic under the sieve zone at different flowrates of the solvent

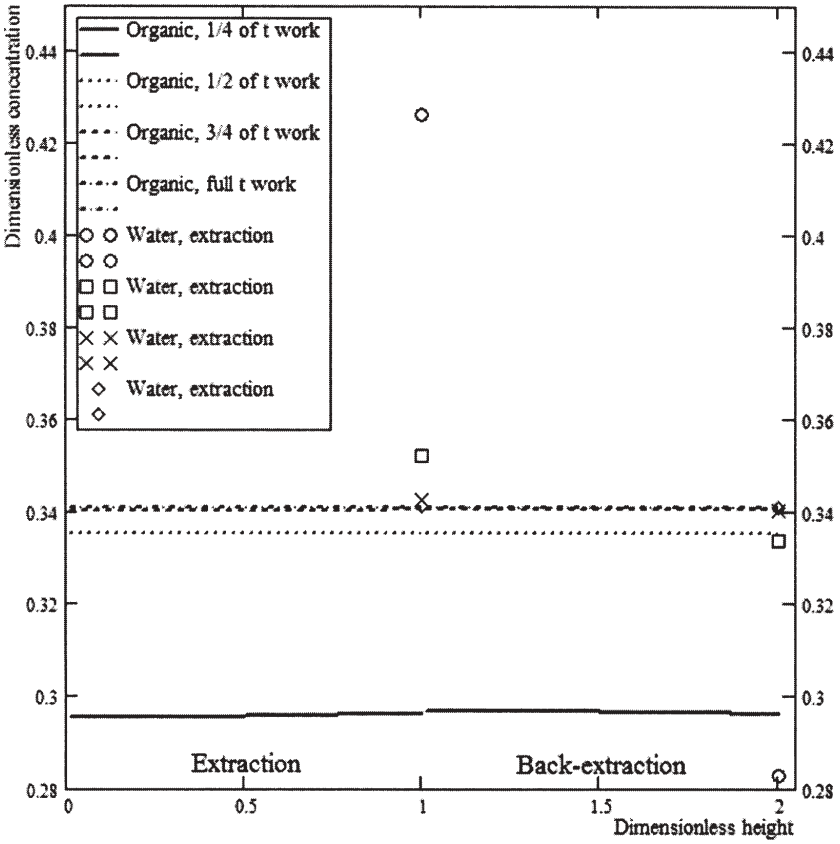

Fig. 5. Transported species concentration profiles along the column in the organic phase for some intermediate values of the batch - the organic flowrate is 0.9 cm^3/s

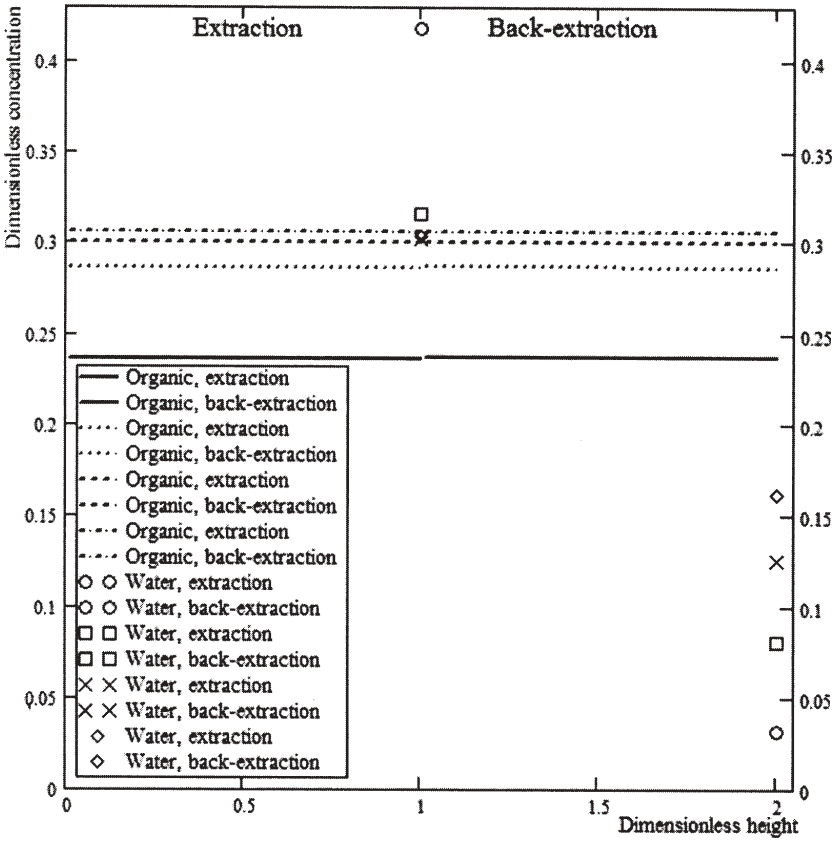

Fig. 6. Transported species concentration profiles along the column in the organic phase for some intermediate values of the batch - the organic flowrate is 0.45 cm^3/s

for the carrier flowrate of 0.9 cm^3/s and figure 6 for 0.45 cm^3/s, respectively. There are four profiles corresponding to time slices taken at one quarter of the overall batch extraction time. It must be emphasized that, since the batch extraction time was set as 150 time greater than the carrier residence time of the system, this value is lower for the higher flowrate (10.53 h) than for the smaller one (20.74 h). So, the time slices were taken at 2.63 h, 5.26 h, 7.89 h and 10.53 for the carrier flowrate of 0.9 cm^3/s and 5.19 h, 10.37 h, 15.55 h and 20.74 h for 0.45 cm^3/s, in that order.

Another observation related to the figures 5 and 6 is that the vertical distance between the same dots stands for the actual overall driving force of the extraction back-extraction process, since they represent the carried species concentration in extractant in the extraction zone and back-extraction, correspondingly.

After one quarter of the overall batch time is gone, the carried species concentration in the organic phase has a rather flat profile, although slightly rising towards the sieve plate (first half of the graph, fig. 5 and 6 corresponding to

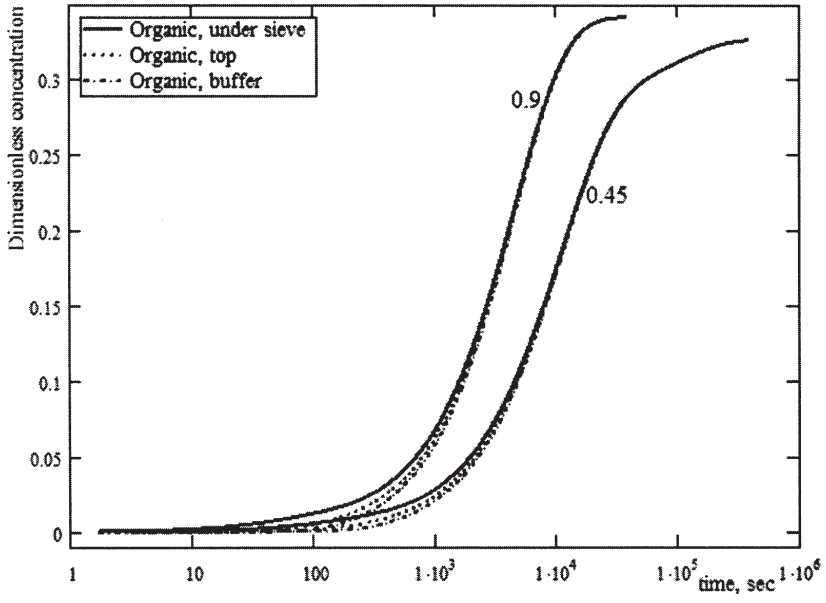

Fig. 7. Concentration profile of the transported species in the perfectly mixed zones (under the sieve, on the top of the column, buffer vessel) at different flowrates of the solvent

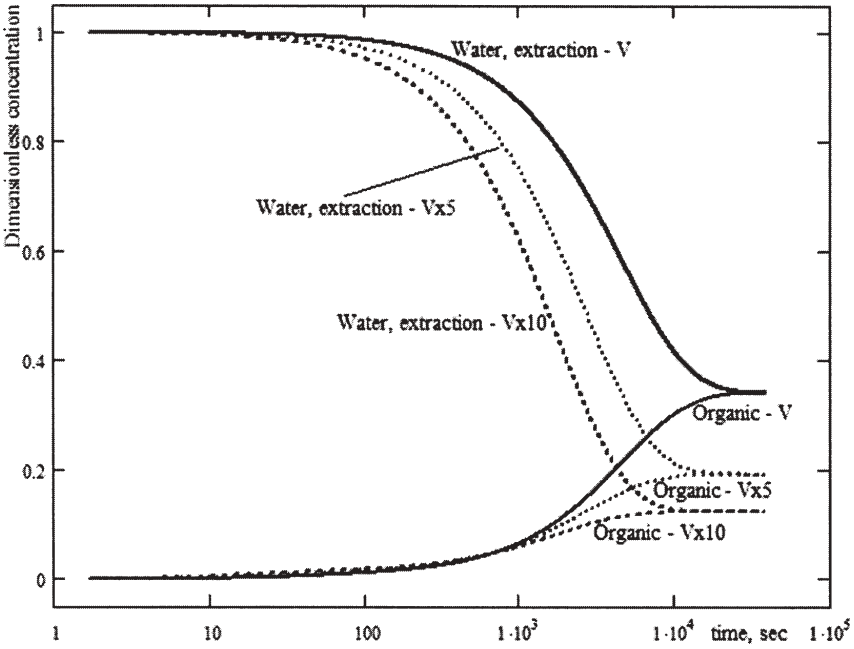

Fig. 8. Concentration profile of the transported species in the continuous phase of the extraction zone and in the organic under the sieve zone at different values of the buffer vessel volume

the extraction zone). This profile is flatter for the smaller flowrate, but this is due simply to the longer period simulation, since in both cases the same carrier residence time for the extraction zone was taken into account (experimentally measured). In the back-extraction zone (second half of the graph, fig. 5 and 6), the concentration profile of the carried species into the organic liquid membrane is slowly decreasing, again less pronounced for the case of smaller flowrate. Due to the supplemental mass transfer from the aqueous phase to the liquid membrane under the sieve, its concentration in carried species becomes higher than that in the incoming droplets. That's why in the back-extraction zone, the carried species has higher concentration, which diminish as the organic liquid membrane approaches the top of the column (second half of the graphs, fig. 5 and 6). It seems that the organic liquid membrane under the sieve acts like an accumulator for the carried species, due to this supplemental mass transfer through its interface with the aqueous phase of the extraction zone. For lower recirculation flows, due to the lower specific mass transfer coefficients, the carried species profiles in the extraction zone become flatter. Once again, there is a commensurable difference between the carried species concentrations in the organic liquid membrane, in favour of the back-extraction zone. For higher time slices, as the overall driving force decreases and the organic membrane becomes richer in carried species, the process reverses, towards the end the carrier in the back-extraction zone having smaller concentrations in the carried species than in the extraction zone (fig. 5 and 6, for the three-quarter of the final time profiles). Eventually, the carrier will have the same concentration in the carried species, corresponding to physical equilibrium, as can be seen from figure 7. Although the overall batch extraction time is higher for the 0.45 cm^3/s carriers flowrate case, this process of reaching equilibrium is lengthier, due to the smaller specific mass transfer coefficients.

Solvent volume

The next parameter whose influence upon the extraction back-extraction process was studied was the solvent volume; the simulation results are shown in figure 8. Analyzing the axial profiles and their associated values, we observe that it is better to work with lowest acceptable

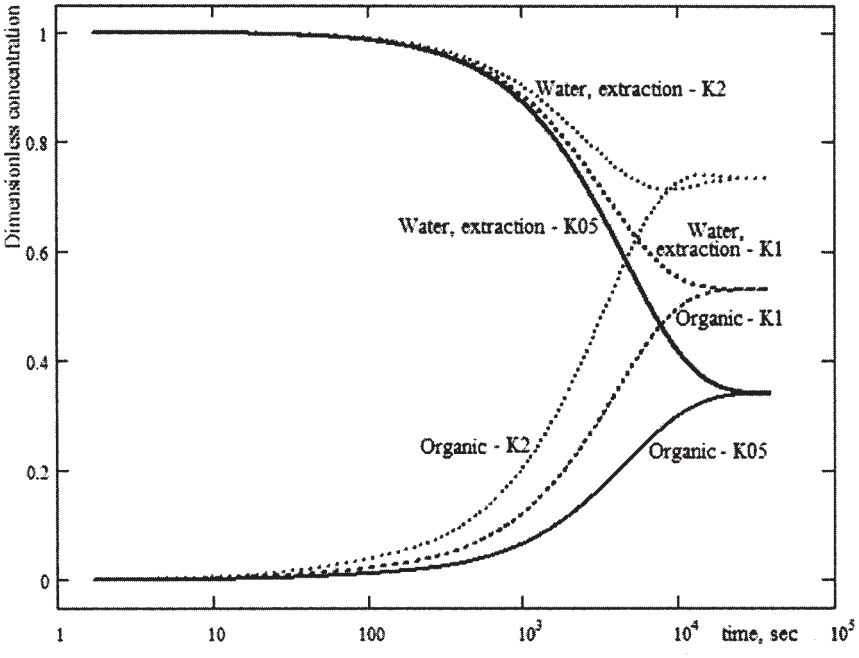

Fig. 9. Concentration profile of the transported species in the continuous phases of the column for different values of the partition coefficient

solvent volumes in the buffer vessel (fig. 1, entry 11). It is true that, as the buffer volume increases, the mass transfer driving force is kept at higher values, since the carried species concentrations is the lowest for the highest working volume, but the drawback is that a larger quantity of the valuable species will be trapped into the organic liquid membrane. This implies a supplemental cost in reclaiming it after the whole process is finished. So, from an economic point of view, there should be an optimum value which increases as the driving force of the mass transfer decreases, balancing the overall extraction costs and the supplemental costs implied by the final separation of the valuable product from the liquid membrane.

Partition coefficient

The last examined parameter, and its effect upon the extraction back-extraction process, was the partition coefficient (K_{eq}^{-1}), which takes into account a change in the organic species used as liquid membrane (equivalently, this could be seen as a change in the carried species, keeping the carrier the same). The simulation results are presented in figure 9. It can be seen that the system tends towards equilibrium faster as the partition coefficient increases, since this means that the organic liquid membrane is capable of extracting faster and at higher concentration the carried species in the extraction zone and release it faster, in the back-extraction zone, since the driving force is higher. The main drawback in using very high partition coefficient organic membranes is that column tends toward an equilibrium at lower and lower concentrations in the back-extraction zone, due to the higher quantities of valuable product entrapped into the organic liquid membrane. Again, this suggests that the whole process can be improved only on economic bases, searching for the appropriate organic to be used as liquid membrane which should balance the benefits of the higher mass transfer capabilities and the higher mass of the retained valuable product.

The influence of the partition coefficient upon the back-extraction process seems to be much less pronounced than for the case of extraction zone. This happens because the mass transfer driving force remains higher, due to the increase in the concentration of the carried species in the organic liquid membrane under the sieve owing to the supplemental mass transfer, which is proportional to the partition coefficient. This increase compensates the decrease in the mass transfer driving force in the back-extraction zone, due to the increase of the carried species concentration in the aqueous phase. If the simulations would had continued for a longer time, the influence of the partition coefficient upon the back-extraction process would have had been more pronounced, since the aforementioned supplement at mass transfer would diminish dramatically.

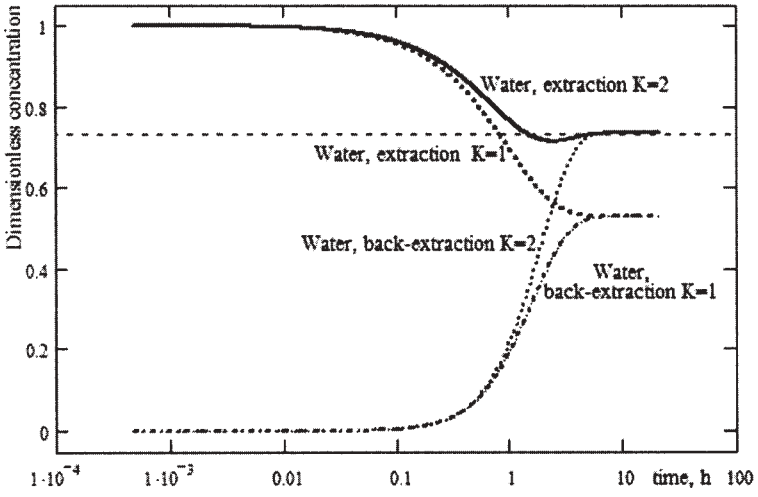

Fig. 10. Concentration profile of the transported species in the continuous phases of the column for high values of the partition coefficient and a very long duration of the process

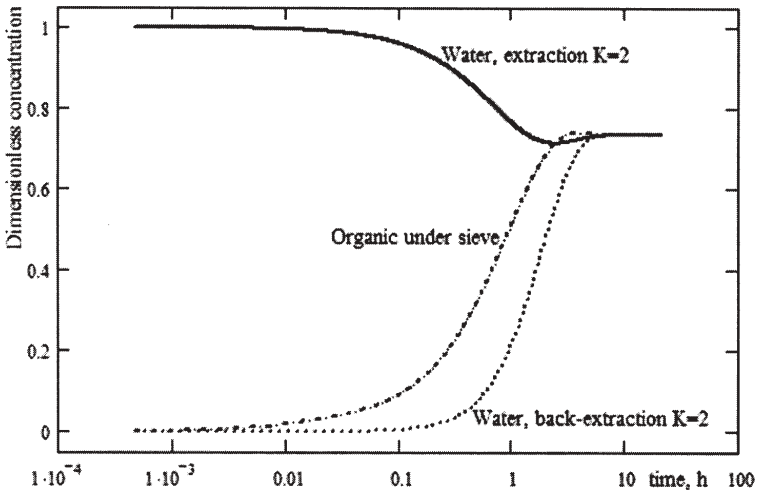

Fig. 11. Concentration profile of the transported species in the continuous phases and organic under the sieve of the column for K = 2 and a very long duration of the process

Organic carrier acting like a reservoir

When the column behaviour is simulated for large partition coefficients and very long operating time, a very interesting phenomenon becomes apparent at the highest carrier flowrate used in this simulation: the mutual dependency of two phenomena having different time-scales, which modify during the process (fig. 9, last time interval, between 10^4 and 10^5 s and fig. 10). When the partition coefficients are large enough, the time scale of the finite mass transfer rate becomes comparable with the rising time of the droplets, which means that the supplemental mass transfer from the extraction zone to the organic under the sieve gains in significance, increasing the later zone's concentration in the carried species significantly. On the other hand, the release of the carried species into the back-extraction zone is rather low, due to the same high values of the large partition coefficients, as can be seen from figure 10, the rising curves corresponding to this zone. In time, the carrier accumulates enough carried species to become a "source" for the both the extraction and the back-extraction zones, till an overall equilibrium is reached (fig. 11 for the time evolution of the carried species in the extraction zone and the organic under the sieve). As depicted in the figure 10, the bigger the partition coefficient, the higher this "reservoir" effect is – see the small minimum in the water concentration in the carried species for K=1, and the larger and more pronounced minimum for K=2 (fig. 10). The same reasoning apply, also, to the situation depicted in figure 3, for the period when the carrier acts like a reservoir.

Conclusions

In this paper a model for a new extraction-back extraction process which develops in a single column is proposed. The extraction and stripping membrane process have been calculated solving a non-linear programming problem. The mathematical model was solved using the orthogonal collocation method, to transform the partial derivatives with respect to space into algebraic terms, thus changing the PDEs into ODEs, with respect to time. In order to validate the model an improved procedure, based upon GA, was used to match the computed and experimental concentration profiles. To eliminate the difficulties associated with the computation of the correct values for the interfacial area between the rising droplets and the stagnant liquid phase, the real adjustable parameters were the specific partial mass transfer coefficients: $k_{o,ex} \cdot A_{ex}$, $k_{A,ex} \cdot A_{ex}$, $k_{o,re} \cdot A_{re}$, $k_{A,re} \cdot A_{re}$. The purposed model accurately describes the process that runs into the experimental device. The operation of the process at different flow rates of the extractant, different volumes of the buffer vessel and different partition coefficients was studied, emphasizing the interdependency of several time scales, whose predominance determines the characteristics of the column operating regime. The numerical results obtained allow issuing appropriate strategies necessary for effective running the extraction at its maximum capability or, as well, determination of the operating parameters for the system at hand. The main benefit of this new mathematical model is its potential use in the designing phase of the extraction back-extraction processes.

Nomenclature

A - interfacial mass transfer area, m^2

C - acid concentration, $kmol/m^3$

D - (equivalent) diameter, m

D_{va} - feed or exit volumetric flow rate of the organic phase, m^3/s

D_v - flow rate of the organic phase, m^3/s

H - height, m

$K_{eq} = \frac{C_A^{eq}}{C_o^{eq}}$ - partition coefficient

k - mass transfer coefficient, m/s

n - average molar flux of the carried species, $kmol/m^2s$

$\bar{t} = \frac{V_t}{D_v}$ - residence time, s

u - organic phase velocity, m/s

V - volume, m^3

z - spatial coordinate, m

Greek letters

τ - dimensionless time

α - residence time fraction corresponding to the extraction zone

β - residence time fraction corresponding to the extraction-back extraction zone

γ - residence time fraction corresponding to the back extraction zone

ψ - residence time fraction corresponding to the top of the column zone

ϕ - residence time fraction corresponding to the buffer vessel

$\delta = \frac{D_{eq}^o}{D_c}$ - diameter ratio;

ξ - dimensionless partial coordinate;

$\Gamma = \frac{C}{C_{A,ex}^{in}}$ - acid dimensionless concentration

Indexes

A- aqueous phase
bk - back-extraction
c - column
eq - equilibrium equivalent
ex - extraction
ex-bk - extraction-back extraction organic buffer zone (zone under the sieve)
f - organic phase from the top of the column
in - initial
o - organic phase
sup - interface under the sieve interface on the top of the column
t - total
v - buffer vessel

References

1. CHAUDHURI, J. B., PYLE, D. L., Chem. Eng. Sci., **47** nr.1, 1992, p. 41
2. YOUNG, S. M., WON, L., KOOK, L., YONG, K., Chem. Eng. J., **66,** 1997, p. 11
3. JUANG, R., HUANG, R., WU, R., J. Membrane Sci., **136,** 1997, p. 89
4. HALWACHS, W. AND SCHÜGERL, K., Int. Chem. Eng., **20** nr.4, 1980, p. 519
5. MORTERS, M., BART, H., Chem. Eng. and Processing, **42,** 2003, p. 801
6. CHAUDHURI, J. B., PYLE, D. L., Chem. Eng. Sci., **47** nr.1, 1992, p. 41
7. BISCAIA JUNIOR, E. C., MANSUR, M. B., SALUM, A., CASTRO, R. M. Z., BRAZ. J. Chem. Eng., **18**, 2001, p. 163
8. ROCKMAN, J. T., KEHAT, E. LAVIE, R., Ind. Eng. Chem. Res., **34** ,1995, p. 2455
9. ELICECHE, A. M., CORVALAN, S. M., ORTIZ, I., Computers and Chem. Eng., **26,** 2002, p. 555
10. NOBLE, R. D., KOVAL, C. A., PELLEGRINO, J. J., Chem. Eng. Progress, **March**, 1989, p.58
11. WEINSTEIN, R., SEMIAT, R., LEWIN, D. R., Chem. Eng. Sci., **53**, 1998, p. 325
12. QUIAN, Y., WANG, J., Can. J. Chem. Eng., **70**, 1992, p. 88
13. SKELLAND, A. H. P., KANEL J. S., Ind. Eng. Chem. Res., **31**, 1992, p. 908
14.DINCULESCU, D., GUZUN-STOICA, A., DOBRE, T., FLOAREA, O., Bioprocess Eng., **22**, 2000, p. 529
15. FINLAYSON, B. A., The method of weighted residuals and variational principles, Academic Press, New York, 1972, p 30
16. VANDERGRAFT, J. S., Introduction to Numerical Computations, Academic Press, New York, 1978, p.54
17. RĂDUCAN, O., LAVRIC, V., WOINAROSCHY, A., Rev. Chim., **55** nr.8, 2004, p. 638
18. LAVRIC, V., IANCU, P., PLE^{a}U, V., J. of Cleaner Production, **13**, 2005, p. 1395
19. OFIÞERU, I. D., WOINAROSCHY, A., LAVRIC, V., European Symposium on Computer Aided Process Engineering-15, May 29 – June 1, Barcelona, Spain, 2005, Computer-Aided Chemical Engineering, **20A** (L. Puigjaner & A. Espuña, Eds.) Elsevier, 2005, p. 775
20. PERRY, R. H., GREEN, D. W., PERRY's Chemical Engineers' Handbook, Mc Graw-Hill, 1999, p.76

Manuscript received: 20.06.2007